Featured Article

Aortic valve opening and closure: the clover dynamics

Emmanuel Lansac[1], Hou-Sen Lim[2], Yu Shomura[2], Khee Hiang Lim[2], Nolan T. Rice[2], Isabelle Di Centa[2], Pouya Youssefi[1,3], Wolfgang Goetz[2], Carlos M. G. Duran[2]

[1]Department of Cardiovascular Surgery, Institut Mutualiste Montsouris, Paris, France; [2]The International Heart Institute of Montana Foundation at St. Patrick Hospital and Health Sciences Center and The University of Montana, Missoula, Montana, USA; [3]Hospital Foch, Suresnes, France
Correspondence to: Emmanuel Lansac, MD, PhD. Department of Cardiovascular Surgery, Institut Mutualiste Montsouris, 42 Bd Jourdan, Paris 75014, France. Email: emmanuel.lansac@imm.fr.

Background: Systolic aortic root expansion is reported to facilitate valve opening, but the precise dynamics remain unknown. A sonometric study with a high data sampling rate (200 to 800 Hz) was conducted in an acute ovine model to better understand the timing, mechanisms, and shape of aortic valve opening and closure.

Methods: Eighteen piezoelectric crystals were implanted in 8 sheep at each annular base, commissures, sinus of Valsalva, sinotubular junction, nodulus of Arantius, and ascending aorta (AA). Geometric changes were time related to pressures and flows.

Results: The aortic root was hemodynamically divided into left ventricular (LV) and aortic compartments situated, respectively, below and above the leaflets. During isovolumetric contraction (IVC), aortic root expansion started in the LV compartment, most likely due to volume redistribution in the LV outflow tract below the leaflets. This expansion initiated leaflet separation prior to ejection (2.1%±0.5% of total opening area). Aortic compartment expansion was delayed toward the end of IVC, likely related to volume redistribution above the leaflets due to accelerating aortic backflow toward the aortic valve and coronary flow reduction due to myocardial contraction. Maximum valve opening during the first third of ejection acquired a truncated cone shape [leaflet free edge area smaller than annular base area (–41.5%±5.5%)]. The distal orifice became clover shaped because the leaflet free edge area is larger than the commissural area by 16.3%±2.0%.

Conclusions: Aortic valve opening is initiated prior to ejection related to delicate balance between LV, aortic root, and coronary dynamics. It is clover shaped at maximum opening in systole. A better understanding of these mechanisms should stimulate more physiological surgical approaches of valve repair and replacement.

Keywords: Aortic valve; aortic root; anatomy; physiology; aortic valve repair

Submitted Feb 01, 2019. Accepted for publication May 03, 2019.
doi: 10.21037/acs.2019.05.03
View this article at: http://dx.doi.org/10.21037/acs.2019.05.03

Introduction

Until recently, aortic valve dynamics were not a concern because prosthetic valve replacement was the standard surgical treatment for aortic valve disease. The increased use of: (I) stentless bioprostheses; (II) aortic valve repair; and (III) valve-sparing procedures all demand a better understanding of aortic valve dynamics (1,2). Although the relationship between the sinuses of Valsalva and the aortic valve had been intuitively shown by Leonardo da Vinci (3), the aortic valve is still regarded as a passive, tri-leaflet structure that moves back and forth according to pressure differences between the left ventricle and aorta. Several authors have questioned this simplistic view by showing that the expansion of the aortic root actively participates in aortic valve opening, reducing shear stress on the leaflets (4-6). However, the underlying mechanism of aortic root expansion prior to valve opening remains unclear. Moreover, the shape of the open aortic valve is still controversial: it has been described as stellate, triangular,

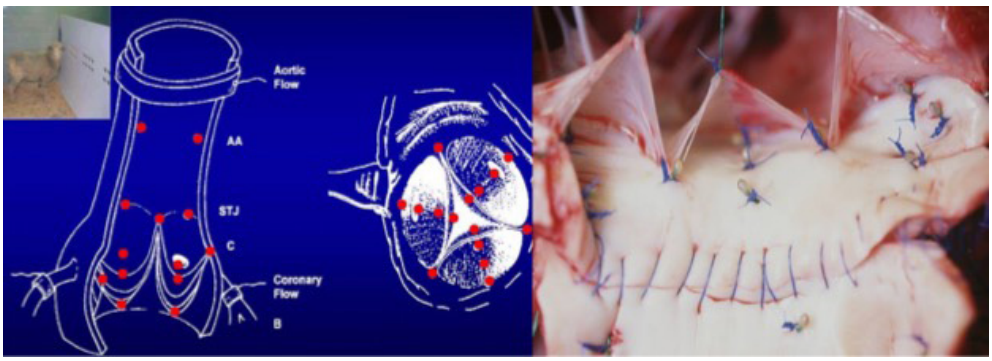

Figure 1 Location of the sonomicrometry crystals in the aortic root. AA, ascending aorta; B, annular base; C, commissures; L, leaflets; SoV, sinus of Valsalva; STJ, sinotubular junction.

and circular (7-9). Most of these studies were limited by a low data sampling rate (60 Hz) that did not allow precise continuous recordings of aortic valve movements. The first step of the present study was to review previously published literature for data obtained using three-dimensional (3D) digital sonomicrometry. This technique is characterized by a high rate of data acquisition (200 to 800 Hz) and offers a unique opportunity for precise examination of the aortic root and valve dynamics within each phase of the normal cardiac cycle (5,10,11). Our analysis focused on the mechanism of aortic root expansion and the shape of the aortic valve orifice at maximum opening.

Methods

Experimental design

Under general anesthesia and cardiopulmonary bypass, 18 ultrasonic crystals were implanted in the aortic root of eight adult Targhee sheep (43±2 kg). The pump time was 158±8 minutes, and the cross clamp time was 75±3 minutes. After the animals were weaned from bypass, recordings were obtained under stable hemodynamic conditions at 200 up to 800 Hz. Epicardial echocardiography was used to assess aortic valve competence. At the end of the experiment, the heart was explanted, and correct position of the crystals was checked.

All animals received humane care in accordance with the *Principles of Laboratory Animal Care*, formulated by the Animal Welfare Act in the National Institutes of Health *Guide for Care and Use of Laboratory Animals* [DHHS Pub. No. (NIH) 85-23, Revised 1996]. The protocol for the use of the animals for this research was also reviewed and approved by the Institutional Animal Care and Use Committee of The University of Montana.

Surgical protocol

Anesthesia was conducted with propofol (4.0 mg/kg). The heart was exposed via a standard left thoracotomy. Because the common brachiocephalic trunk arises from the ascending aorta (AA) very early in sheep, the left femoral and internal thoracic arteries were cannulated. This made it possible to simultaneously cross clamp both the arch and brachiocephalic artery without inducing brain ischemia. Venous return was established with a 32-Fr dual stage single cannula (Medtronic Inc., Minneapolis, MN, USA). After initiation of cardiopulmonary bypass, the AA was cross-clamped and cold blood cardioplegia was infused.

Eighteen 1-mm ultrasonic crystals (Sonometrics Corporation, London, Ontario, Canada) were implanted and secured with a 5/0 polypropylene suture through a transverse aortotomy approximately 1 cm distal to the sinotubular junction (STJ). Three crystals were secured at each of the following levels: the nadir of each leaflet or annular base (B:3); the commissures (C:3); the highest point of each supra-aortic crest or STJ (STJ:3); and at the wall of the AA (AA:3) (*Figure 1*). All electrodes of the crystals were exteriorized through the aortic wall at their point of insertion to reduce possible interference with valve movements. Three smaller, 0.7 mm crystals were sutured to each nodulus of Arantius (L:3), and their electrodes were exteriorized through the aortotomy. In four sheep, 1 mm crystals were placed on the concavity (deepest point) of the three sinuses of Valsalva (SoV:3). High-fidelity, catheter-tipped pressure transducers (model 510, Millar Instruments, Houston, TX, USA) were placed in the lumen of the

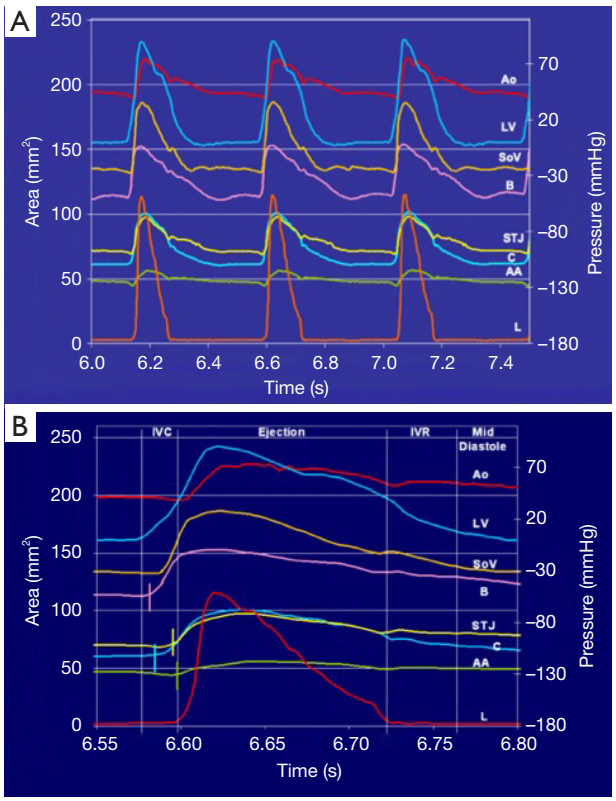

Figure 2 Changes at each level of the aortic root time related to left ventricular (LV) and ascending aorta (AA) pressures (sheep 7). Leaflet (L) free edge area exceeds commissural (C) and sinotubular (STJ) areas (clover-shaped orifice) but is never larger than annular base (B) and sinuses of Valsalva (SoV) areas (cone-shaped). Ao, aortic pressure. (A) 3 cycles; (B) 1 cycle.

proximal AA and in the left ventricular (LV) cavity. Flow meter rings (model T206, Transonic Systems, Ithaca, NY, USA) were placed around the AA and the proximal right and left main coronary arteries. Recordings were obtained after the animal was hemodynamically stable (minimum post-pump time of 30 minutes). At the conclusion of the experiment, the animal was euthanized with an i.v. bolus of propofol and 20 mEq of potassium chloride.

Definition of the cardiac cycle phases

The geometric changes were time related to each phase of the cardiac cycle defined from the aortic and LV pressure curves (*Figure 2*) (12). End diastole, or beginning of isovolumetric contraction (IVC), was defined as the point of LV pressure increase. End of IVC was defined as the beginning of ejection at the crossing point of the LV and aortic pressure curves. The dicrotic notch in the aortic pressure curve defined end ejection. End of isovolumetric relaxation (IVR), or the initial phase of diastole, was defined as the lowest point of LV pressure after ejection (13).

Definition of anatomic aortic root regions

The aortic root and the AA were divided into five cross-sectional areas each defined by three crystals: annular base (B), sinus of Valsalva (SoV), commissural (C), STJ, and AA (*Figure 1*). The area between the three leaflet crystals placed on the nodulus of Arantius defined the aortic valve orifice.

Data acquisition and calculation of aortic root deformation

Distances between crystals were measured with a digital ultrasonic measurement system (TRX Series, Sonometrics Corporation, London, Ontario, Canada). A post-processing program (Sonometrics Corporation, London, Ontario, Canada) was used to examine each individual distance between crystals and for 3D reconstruction of the crystal coordinates. Recordings of pressures, flows, and distances between crystals were synchronized on the same timeline.

Data were obtained directly from the measured distances between pairs of crystals, and Lagrangian strain was used to define the deformation from the original distance at end diastole (strain, S was defined as the ratio of the change in length of a line segment, a to its initial length, b: $S = a/b$). Each level of the aortic root was represented by a triangular area defined from the three corresponding crystals and calculated using the Heron formula (14). The Sonovol post-processing program (Sonometrics Corporation, London, Ontario, Canada) was used to calculate aortic root volumes using the convex hull approach (2). Crystals at the basal, commissural, and STJ levels were used for these calculations.

Changes in length, area, and volume were defined by: (I) total expansion as the percentage change with reference to the original value at end diastole; and (II) proportional expansion as the percentage changes during each phase of the cardiac cycle relative to the total changes over the entire cycle.

Measurement and statistical analysis methods

After close examination of the data, three consecutive

Table 1 Phase-related changes at each level of the aortic root for each phase of the cardiac cycle

Variable	IVC	Ejection (first third)	Ejection (last two-thirds)	IVR	Mid diastole	End diastole	Total expansion
B % change in area	50.7±4.5*	49.2±4.5*	−54.4±2.0*	−44.1±3.8*	−18.9±1.5*	17.5±3.0*	29.8±3.3**
B raw area (cm^2)	1.45±0.12	1.63±0.09	1.45±0.11	1.30±0.12	1.24±0.12	1.29±0.12	1.29–1.63
SoV % change in area	35.8±4.8*	64.2±4.8*	−74.9±3.8*	−31.0±2.2*	−6.3±1.5*	12.2±2.4*	38.4±1.1**
SoV raw area (cm^2)	1.44±0.08	1.76±0.07	1.40±0.08	1.24±0.07	1.21±0.06	1.27±0.04	1.27–1.76
C % change in area	32.8±3.2*	67.1±3.2*	−66.6±1.4*	−29.4±1.2*	−8.6±1.1*	4.7±0.9*	63.7±3.6**
C raw area (cm^2)	0.72±0.05	0.98±0.05	0.73±0.04	0.62±0.04	0.59±0.04	0.60±0.03	0.60–0.98
STJ % change in area	13.8±1.9*	86±1.9*	−68±2.6*	−14.2±2.3*	−17.5±2.7*	−0.2±0.6*	37.1±2.1**
STJ raw area (cm^2)	0.65±0.07	0.85±0.09	0.70±0.08	0.67±0.08	0.62±0.07	0.62±0.07	0.62–0.85
AA % change in area	6.6±1.0*	93.3±1.0*	−64.3±3.0*	−10.9±3.2*	−18.2±3.6*	−6.4±2.4*	26.3±0.9**
AA raw area (cm^2)	0.60±0.09	0.74±0.10	0.64±0.09	0.63±0.09	+0.60±0.09	0.59±0.09	0.59–0.74
L % change in area	2.1±0.8	97.9±0.8	−99.1±0.2	−0.9±0.2	0.0±0.0	0.0±0.0	100±0.0
L raw area (cm^2)	0.06±0.02	1.20±0.03	0.98±0.06	0.05±0.005	0.00	0.00	0.00–1.20
Ao root volume (%)	36.7±3.3*	63.3±3.3*		−39.1±3.6*	−19.0±2.4*	11.3±2.4*	33.7±2.7**

Data are reported as percentage of area changes for each phase of the cardiac cycle relative to the total changes over the entire cycle. They are followed by the raw area value measured at the end of each phase of the cardiac cycle. Results are expressed as mean plus or minus one standard error of the mean. *, P<0.05, proportional percentage area changes during each phase of the cardiac cycle is statistically significant relative to the total area changes over the entire cycle; **, P<0.05, total percentage area change is statistically significant with reference to the original value at end diastole. IVC, isovolumic contraction; IVR, isovolumic relaxation; AA, ascending aorta; B, annular base; C, commissures; L, leaflets; SoV, sinus of Valsalva; STJ, sinotubular junction; Ao, aortic.

heartbeats that contained the least amount of noise were chosen for analysis. The summary statistics are reported as mean plus or minus one standard error of the mean (mean ±1 SEM). Area changes at each level of the aortic root and valve orifice were tested for significance using the Student *t*-test for paired observation (significance level P<0.05). Pearson correlations were studied to measure the degree of linear relationship between area expansion and pressure increase. All statistical analyses were done using the SPSS 0.9 program (SPSS, Inc., Chicago, IL, USA).

Results

The hemodynamic parameters at the time of data acquisition were: heart rate 145±8 beats per minute; aortic pressure 70/45±5/4 mmHg; stroke volume 20±2 mL; and cardiac output 2.8±0.3 L/min. Seven sheep had no regurgitation, and one had trivial regurgitation on epicardial echocardiography. Necropsy showed the crystals in the correct position.

The aortic valve dynamics were closely related to the aortic root volume expansion, which increased by 33.7%±2.7% during systole. According to root volume changes, results are presented in these six critical phases of the cardiac cycle: IVC, first third of ejection, last two-thirds of ejection, IVR, mid-diastole, and end diastole (*Table 1*, *Figure 2*).

Aortic root expansion and valve opening are initiated prior to ejection

Aortic root expansion started prior to ejection. Of the total aortic root volume increase, 36.7%±3.3% occurred during IVC. During this phase, the aortic root started to expand at its base and commissures, followed by the STJ, and then the AA (*Figure 2*). In proportion, the expansion of the root was greater at the annular base and commissures levels than at the STJ and AA levels (*Figure 3*). Expansion of the annular base and commissures was strongly related with LV pressure increase (r=0.95). This expansion probably

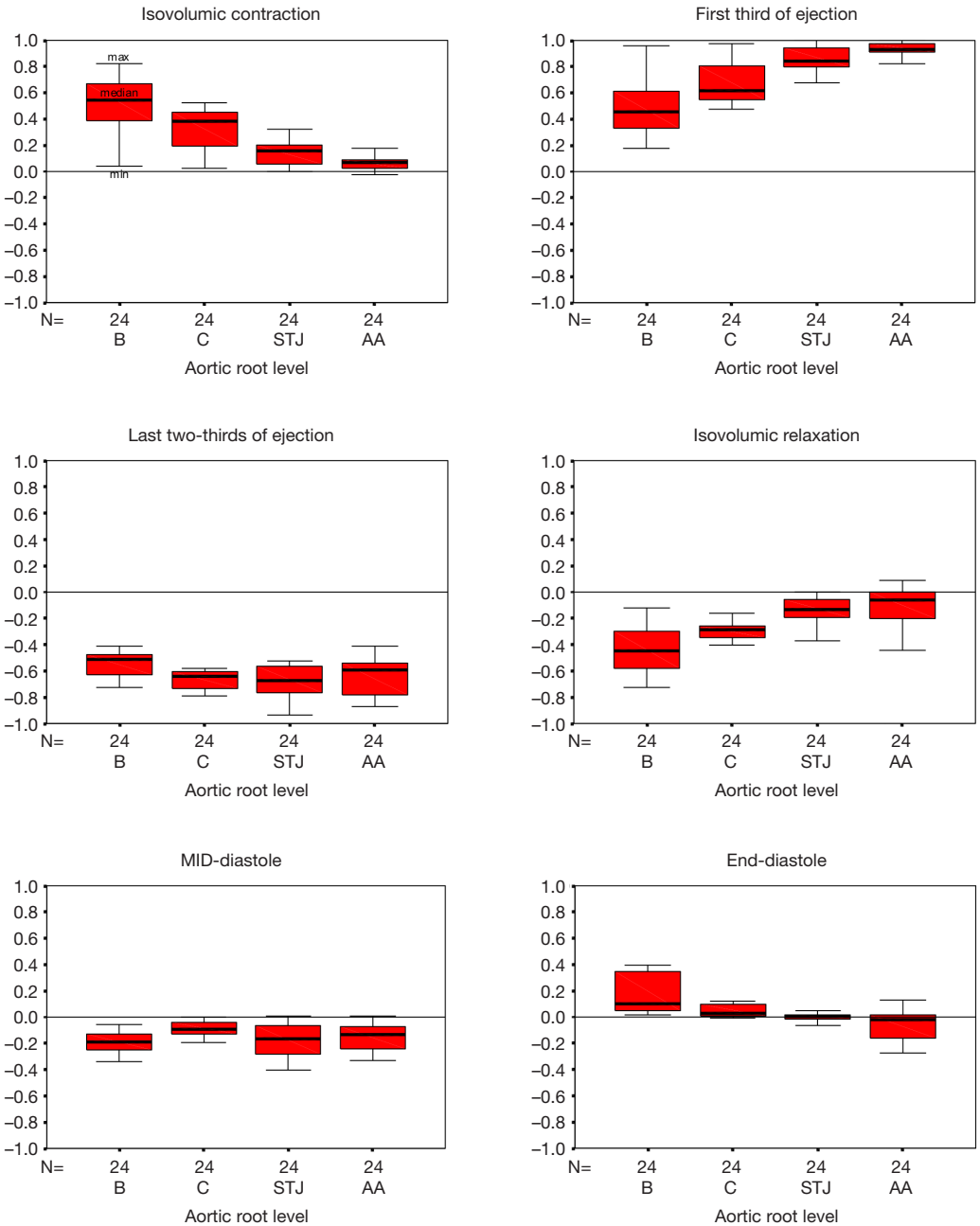

Figure 3 Area changes during the cardiac cycle at each level of the aortic root displayed in side-by-side box plot. B, base; C, commissures; STJ, sinotubular junction; AA, ascending aorta.

corresponds to LV blood volume redistribution in the LV outflow tract, below the leaflets, during IVC (*Table 2*, *Figure 4*).

The expansion of the STJ and AA was delayed toward the end of the isovolumetric phase and was not related to LV pressure or aortic pressure. It might be related to a redistribution of volume above the leaflets due to accelerating backflow in the AA toward the aortic valve (57.4±16.4 mL/s^2) as ejection has not started yet while coronary flow is reduced (main left: −47.2±3.7 mL/s^2, right: −13.6±3.1 mL/s^2) due to myocardial contraction.

These findings suggest that the aortic root is divided

Table 2 Pressure-related correlations of area expansion at each level of the aortic root during IVC and ejection

Variable	IVC		Ejection	
	LV pressure	Ao pressure	LV pressure	Ao pressure
AA	−0.49 (−0.92–0.51)	0.72 (0.33–0.96)	0.68 (0.53–0.94)	0.94 (−0.88–0.99)*
STJ	0.14 (−0.93–0.94)	0.14 (−0.63–0.72)	0.93 (0.83–0.97)*	0.86 (0.65–0.98)*
C	0.95 (0.86–0.99)*	−0.38 (−0.91–0.53)	0.95 (0.84–0.99)*	0.80 (0.63–0.93)
B	0.95 (0.88–0.98)*	−0.44 (−0.96–0.53)	0.91 (0.79–0.98)*	0.52 (0.3– 0.78)

*, significant correlation. IVC, isovolumic contraction; LV, left ventricular; Ao, aortic; AA, ascending aorta; STJ, sinotubular junction; C, commissures; B, annular base.

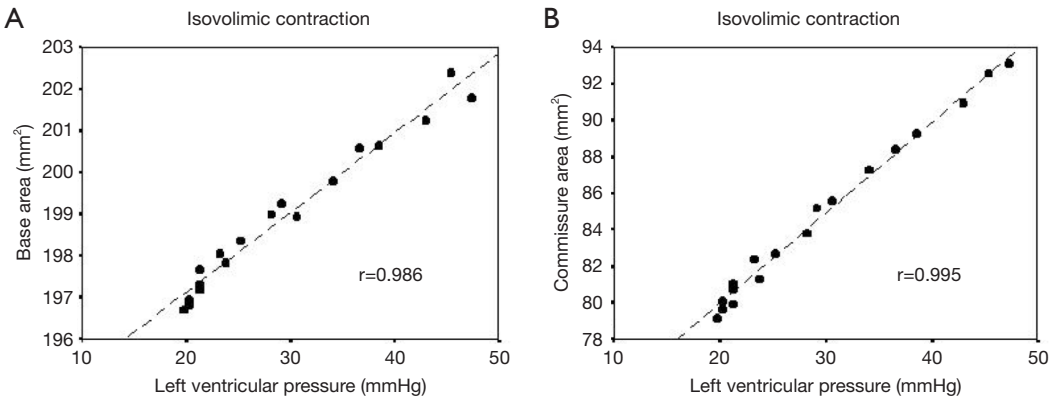

Figure 4 Pearson correlation between basal (A) and commissural (B) areas and left ventricular pressure during IVC. Scatterplot of sheep 7. The least squares linear regression line is added for illustration. IVC, isovolumetric contraction.

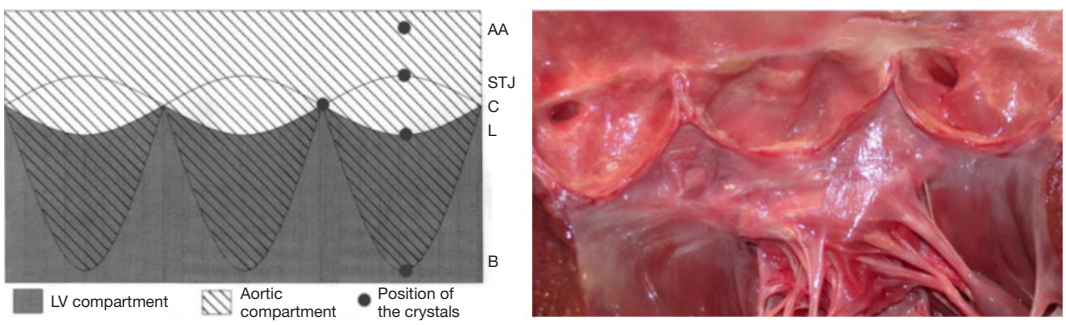

Figure 5 Diagram of the bi-compartmental structure of the aortic root. B, base; L, leaflets; C, commissures; STJ, sinotubular junction; AA, ascending aorta; LV, left ventricle.

into two compartments (*Figure 5*). The first is an LV compartment situated below the leaflets that includes the sigmoid-shaped line of attachment of the leaflets (aortic annulus), the interleaflet triangles, and the commissures; this compartment is related to LV hemodynamics. The second compartment is called the aortic compartment. It is situated above the leaflets and includes the STJ and the AA. It is related to aortic and coronary flow dynamics.

The LV compartment expansion during IVC initiated aortic leaflet separation by 2.1%±0.5% prior to ejection

Table 3 Ratio between maximum leaflet orifice and simultaneous area expansion at each aortic root level

Variable	B	SoV	C	STJ
Leaflet area ratio at maximal opening	–41.5%±5.5%	–54.4%±2.7%	16.3%±2.0%	28.8%±3.4%

Results are expressed as mean plus or minus one standard error of the mean. B, annular base; SoV, sinus of Valsalva; C, commissures; STJ, sinotubular junction.

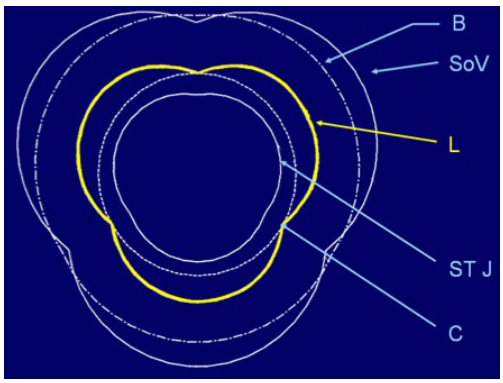

Figure 6 Illustrative cross-sectional area diagram of the aortic root at maximum expansion during ejection. Note the clover-shaped orifice of the aortic valve. C, commissures; STJ, sinotubular junction; L, leaflets; SoV, sinus of Valsalva; B, base; AA, ascending aorta.

while the aortic pressure was still higher than the LV pressure (pressure gradient LV-aorta =–8.5±2.6 mmHg). The three leaflets of the aortic valve (studied at 800 Hz) did not open at the same time. Although the order was consistent for each sheep, no general pattern was found. The aortic root achieved its maximum volume expansion during the first third of ejection (*Figures 2,3*). The expansion of the aortic annulus (LV compartment) was strongly related to the LV pressure increase; aortic compartment expansion was strongly related to the aortic pressure increase. As soon as the aortic valve was open, the expansion of the STJ became related to both pressures (LV: r=0.93; aortic: r=0.86) (*Table 2*).

Aortic valve opening was maximal during the first third of ejection. While the area formed by the leaflet free edges was always smaller than the area of the annular base (–41.5%±5.5%), the free edge area exceeded the commissural area expansion by 16.3%±2.0% (*Table 3*). Therefore, at maximum opening, the aortic valve acquired a truncated cone shape with a clover-shaped distal orifice. Based on this confrontation between the calculated triangular area and the anatomical statement of cross section of the root at each level, an illustrative diagram was designed (*Figure 6*).

Aortic valve closure starts during ejection

Aortic leaflet closure was sharp and started during the last two-thirds of ejection (*Figure 2*) while the aortic root volume decreased. At closure time, the aortic pressure was higher than the LV pressure (gradient: –13.2±1.5 mmHg). Both compartments of the aortic root started to decrease during the last two-thirds of ejection until mid-diastole (*Figure 2*). During end diastole, the root volume re-increased in relation to LV compartment re-expansion (basal area: 17.5%±3.0%; commissural area: 4.7%±0.9%), corresponding to LV filling. Simultaneously, the aortic compartment kept decreasing (STJ area: –1.5%±0.6% and AA area: –6.4%±2.4%), corresponding to aortic pressure decrease before a new ejection phase (*Table 1*, *Figure 3*).

Discussion

The aortic valve is generally understood as a simple trileaflet structure that passively opens and closes according to pressure changes between the LV and aorta. This concept has led to the development of all mechanical and stented bioprostheses. However, in 1976, Brewer *et al.* (4) described the interdependence of aortic valve opening and root expansion in an isolated aortic root model. They showed that valve opening was related to the 16% radial displacement of the commissures, which was interpreted as a mechanism to reduce shear stress on the leaflets. Using radio-opaque markers in dogs, Thubrikar *et al.* (6,8) confirmed *in vivo* that valve opening was related to commissural expansion prior to ejection. They suggested that the mechanism of valve opening was related to the release of the inward pull of the commissures that occurs during IVC. Although they did not measure it, they also suggested that the constraining effect of the annular base was part of the mechanism. Limited by their data-

sampling rate (60 Hz), all calculations were made on abnormal cardiac cycles under the assumption that a non-ejecting extra systole was equivalent to the IVC. Similarly, Vesely (11) interpreted aortic root dilation prior to valve opening to be secondary to passive hemodynamic recoil of the aortic root.

Our findings precisely identify the significant aortic root expansion during IVC that initiates the aortic leaflet separation prior to ejection. This opening is primarily due to commissural expansion, but it is also due to the expansion of the annular base (both are strongly related to the LV pressure increase during IVC). These findings also confirm the study of Sutton *et al.* (15), who described the interleaflet triangles—located under the semilunar attachment of the leaflets—as an essential component of the aortic annulus and part of the LV outflow tract.

Indeed, the present data strongly underline the notion that the aortic root is a junction between the LV and the systemic circulation. The thin leaflets separate two compartments with different hemodynamic systems. The first, LV compartment, is situated below the leaflets and includes the sigmoid-shaped leaflet attachments (traditionally described as the annulus), the interleaflet triangles, and the commissures. These structures are related to the LV hemodynamics. The second, aortic compartment, is situated above the leaflets, includes the STJ and AA, and is related to aortic and coronary flow dynamics. During IVC, aortic root expansion starts at the LV compartment—probably due to volume redistribution in the LV outflow tract. Recently, Rodríguez *et al.* (16) quantified these interventricular volume shifts and demonstrated that they occur during IVC.

The aortic compartment expansion is delayed at the end of IVC due to a redistribution of volume above the leaflets. Confirmation of these bi-compartmental volume dynamics is provided during end-diastole, by the observed re-expansion of the aortic root related to LV compartment expansion during LV filling.

The initiation of leaflet separation (i.e., valve opening) is a dynamic process that occurs in the presence of a negative LV-aorta pressure gradient (–8.5±2.6 mmHg) during an extremely short period of time at end IVC just before ejection starts which did not allow time for aortic regurgitation to occur. This finding contradicts the report of Green *et al.* (17), who stated that, "aortic valve opening began when the trans-valvular pressure gradient had reached maximum (12±5 mmHg)." Difference can be explained by the low data-sampling rate of 0.0167 s (60 Hz) used in that study where most likely the end of IVC have been integrated into the first third of ejection or not recorded.

The shape of the aortic valve orifice remains speculative. Thubrikar *et al.* (6,8,9), followed by Higashidate *et al.* (7), described it as initially stellate, then triangular and circular at maximal opening. These studies were limited by their low data sampling rate (60 Hz), which did not allow for a continuous recording of the changes in valve orifice within each phase of the cardiac cycle. Our data sampling rate of 200 to 800 Hz showed that the shape of the aortic valve orifice progressed from initially stellate to triangular then circular and finally clover shaped at maximum opening. At that time, the leaflet's free edge area exceeded the commissural area by 16.3%±2.0%. Our findings correlate well with phase-contrast flow MRI studies which show systolic 3D velocity profiles exiting the aortic valve to be clover-shaped in healthy tricuspid aortic valve volunteers (18,19). This behavior of the valve leaflets might explain cases of early leaflet deterioration following re-implantation of the aortic valve within a tubular conduit without sinuses of Valsalva (2,20). Leaflet expansion beyond the commissural level would result in leaflet impact against the wall of the cylindrical conduit. At maximum opening, the valve formed a truncated cone starting from the annular base up to the free edge of the leaflets. Indeed, the expansion of the leaflet's free edge area was never larger than the expansion at the aortic annular base. This funnel shape might maximize hemodynamic performance by directing flow through the sinotubular orifice, which was the smallest orifice of the aortic root at all times and could therefore be considered the effective aortic orifice toward systemic circulation. The systolic cone shape of the valve with a distal clover shaped orifice larger than the sinotubular orifice can be interpreted as an efficient mechanism to direct flow toward the supra-aortic crests, facilitating the formation of vortices within the sinuses of Valsalva. These vortices were described by Leonardo da Vinci (3), shown *in vitro* by Bellhouse (21), and more recently visualized *in vivo* in humans with magnetic resonance (22). They initiate valve closure during ejection in order to avoid valve regurgitation.

Indeed, MRI and computational fluid dynamics studies have shown that as well as leaflet impact on a cylindrical conduit, there are further deleterious haemodynamic effects in using a straight cylindrical conduit. Ranga *et al.* compared remodeling and reimplantation techniques using an MRI-derived computational model (23). They found a

loss of vortex formation at peak systole with the straight cylinder reimplantation technique, whereas the remodeling procedure reproduced the vortices seen in healthy volunteers. Furthermore, the flow pattern between the cylinder wall and the cusps which initiates valve closure was more flat and horizontal in the reimplantation technique than in the remodeling or control models (where it was more vertical), which may explain the rapid valve closure seen in the reimplantation technique. Kvitting *et al.* used MRI in healthy volunteers to show that vortices gradually increase in size within the sinuses as aortic velocities decrease, and that these vortices persist into diastole (24). However, these vortices were not seen in their patients following reimplantation root replacement with a straight cylinder. These studies were in contrast to Markl *et al.* who showed that some vortex formation was seen in straight cylinder reimplantation technique, however, vortices were increased with a modification of the technique which created a bulb-shaped root (25).

As a result of concerns regarding the hemodynamics of a straight cylinder graft used to replace the root in the reimplantation technique, a bulb-shaped graft has been developed and used more recently for root replacement techniques (including both reimplantation and remodeling). Oechtering *et al.* used 4D MRI to evaluate flow patterns following reimplantation using these grafts (26). They found that vortex formation was present in patients following reimplantation with the bulb-shaped graft, and the vortices had similar configuration compared to healthy volunteers. But interestingly, vortices formed following the reimplantation procedure were larger in size than those in healthy volunteers. This may be in part due to the difference in root shape created when using these grafts with the reimplantation and remodeling techniques. In the remodeling technique, the bulb-shaped graft is scalloped to create three separate sinuses which are anastomosed to the aortic root, thereby creating a neo-root which has three distinct bulge-shaped sinuses similar to its native anatomy. However, in the reimplantation technique, the aortic root is anastomosed inside the bulb-shaped graft, thereby creating a spherical neo-root. This may explain why vortices formed with the bulb-shaped reimplantation technique are larger than normal. It is unclear at this stage what the clinical relevance of vortex size is—however, one can theorize that too small vortices lead to leaflet collision with the vessel wall, whereas too large vortices lead to kinetic energy loss and increased strain on the left ventricle (27).

Furthermore, as previously published (13,28), aortic root expansion is asymmetric and induces a tilting dynamic of the aortic valve throughout the cardiac cycle aligning the LV outflow tract with the AA during systole in order to maximize ejection. As soon as the valve starts closing, the angle tilts back as a shock absorber, reducing stress on the leaflets.

The present findings should have important clinical relevance in both directing the surgical techniques of valve repair and in the design of new prostheses. In both cases, their durability will depend on their ability to mimic aortic root function. These types of surgeries should take into account the following physiological facts: (I) the aortic valve and root undergoes significant and continuous geometric changes during the cardiac cycle. Therefore, all structures should be flexible. (II) The tilting angle of the root probably facilitates ejection and reduces stress. (III) The sinuses of Valsalva are essential components for the physiological movements of the aortic leaflets. They make possible the full excursion of the leaflets, resulting in a clover-shaped maximum orifice. Therefore, any valve sparing procedure that abolishes the sinuses of Valsalva should be discarded. Even when a reimplantation technique uses a prosthetic tube with sinuses of Valsalva, the aortic annulus and intertrigonal triangles remain within the prosthesis, impairing their dynamics (2,28). The combination of remodeling the root with an expansible subvalvular annuloplasty might offer a more physiological reconstruction of the aortic root (29-32).

Limitations of the study

The main limitation of this study is the acute, open-chest nature of our model, which might have altered the hemodynamic conditions at the time of data collection. Even so, the constant patterns found in all animals add to the validity of our findings. Another limitation of the study is the possible interference on the valve movements by the presence of the sonometric crystals and electrodes. No electrode traversed the valve orifice, and all but the leaflet electrodes were exteriorized through the wall at their point of insertion. Variability in the location of the crystals was minimized by their implantation by a single investigator.

Conclusions

The aortic valve can no longer be understood as a passive trileaflet structure. Aortic valve opening is initiated prior to ejection related to root expansion with a clover shaped orifice at maximum opening in systole. Mechanisms of

its opening and closure result from a delicate balance between LV, aortic root, and coronary dynamics, ensuring its durability throughout life. Although the use of sonomicrometry has improved our understanding of the physiology of the aortic root, we predict that newer imaging technologies will further disclose the efficient intricacies of this apparently simple structure. The quest for further understanding must continue, and it should stimulate development of more physiologically based valve-sparing procedures that spare not only the valve but also the dynamics of the aortic root as a whole.

Acknowledgments

We wish to thank Kathleen Billington and Leslie Trail for their effort and support, which were essential to the completion of these experiments. We also thank Dr. Isabelle Di Centa and Jill Roberts for their editorial assistance and Reed Mandelko for the illustrations.

Footnote

Conflicts of Interest: The authors have no conflicts of interest to declare.

References

1. David TE, Feindel CM. An aortic valve-sparing operation for patients with aortic incompetence and aneurysm of the ascending aorta. J Thorac Cardiovasc Surg 1992;103;617-21.
2. Leyh RG, Schmidtke C, Sievers HH, et al. Opening and closing characteristics of the aortic valve after different types of valve-preserving surgery. Circulation 1999;100:2153-60.
3. Robicsek F. Leonardo da Vinci and the sinuses of Valsalva. Ann Thorac Surg 1991;52;328-35.
4. Brewer RJ, Deck JD, Capati B, et al. The dynamic aortic root: its role in aortic valve function. J Thorac Cardiovasc Surg 1976;72;413-7.
5. Pang DC, Choo SJ, Luo HH, et al. Significant increase of aortic root volume and commissural area occurs prior to aortic valve opening. J Heart Valve Dis 2000;9;9-15.
6. Thubrikar M, Harry L, Nolan SP. Normal aortic valve function in dogs. Am J Cardiol 1977;40;563-8.
7. Higashidate M, Tamiya K, Toshiyuki B, et al. Regulation of the aortic valve opening: in vivo dynamic of aortic valve orifice area. J Thorac Cardiovasc Surg 1995;110;496-503.
8. Thubrikar M, Bosher LP, Nolan SP. The mechanism of opening of the aortic valve. J Thorac Cardiovasc Surg 1979;77;863-70.
9. Thubrikar MJ, Heckman JL, Nolan SP. High speed cine-radiographic study of the aortic valve leaflet motion. J Heart Valve Dis 1993;2:653-61.
10. Gorman JH 3rd, Gupta KB, Streicher JT, et al. Dynamic three-dimensional imaging of the mitral valve and the left ventricle by rapid sonomicrometry array localization. J Thorac Cardiovasc Surg 1996;112;712-26.
11. Vesely I. Aortic root dilation prior to valve opening explained by passive hemodynamics. J Heart Valve Dis 2000;9:16-20.
12. Guyton AC, Hall JE. Textbook of Medical Physiology, 9th ed. Philadelphia, PA: WB Saunders, 1996:110-5.
13. Dagum P, Green GR, Nistal FJ, et al. Deformational dynamics of the aortic root: modes and physiologic determinants. Circulation 1999;100;II54-62.
14. Pappas T. "Heron's Theorem." The Joy of Mathematics. San Carlos, CA: Wide World Publishing/Tetra, 1989:62.
15. Sutton JP, Ho SY, Anderson RH. The forgotten interleaflet triangles: a review of the surgical anatomy of the aortic valve. Ann Thorac Surg 1995;59;419-27.
16. Rodríguez F, Green GR, Dagum P, et al. Left ventricular volume shifts and aortic root expansion during isovolumic contraction. J Heart Valve Dis 2006;15:465-73.
17. Green GR, Dagum P, Timek TA, et al. The mechanism of aortic valve opening in an ovine model [abstract]. Circulation 1999;Suppl I:I-363, #1906.
18. Youssefi P, Gomez A, He T, et al. Patient-specific computational fluid dynamics-assessment of aortic hemodynamics in a spectrum of aortic valve pathologies. J Thorac Cardiovasc Surg 2017;153:8-20.e3.
19. Youssefi P, Gomez A, Arthurs C, et al. Impact of Patient-Specific Inflow Velocity Profile on Hemodynamics of the Thoracic Aorta. J Biomech Eng 2018. doi: 10.1115/1.4037857.
20. Gallo R, Kumar N, Al Halees Z, et al. Early failure of aortic valve conservation in aortic root aneurysm. J Thorac Cardiovasc Surg 1995;109;1011-2.
21. Bellhouse B, Bellhouse F. Fluid mechanics of model normal and stenosed aortic valves. Circulation Res 1969;25;693-704.
22. Kilner PJ, Yang GZ, Wilkes AJ, et al. Asymmetric redirection of flow through the heart. Nature 2000;404;759-61.
23. Ranga A, Bouchot O, Mongrain R, et al. Computational simulations of the aortic valve validated by imaging data:

evaluation of valve-sparing techniques. Interact Cardiovasc Thorac Surg 2006;5:373-8.
24. Kvitting JP, Ebbers T, Wigstrom L, et al. Flow patterns in the aortic root and the aorta studied with time-resolved, 3-dimensional, phase-contrast magnetic resonance imaging: implications for aortic valve-sparing surgery. J Thorac Cardiovasc Surg 2004;127:1602-7.
25. Markl M, Draney MT, Miller DC, et al. Time-resolved three-dimensional magnetic resonance velocity mapping of aortic flow in healthy volunteers and patients after valve-sparing aortic root replacement. J Thorac Cardiovasc Surg 2005;130:456-63.
26. Oechtering TH, Hons CF, Sieren M, et al. Time-resolved 3-dimensional magnetic resonance phase contrast imaging (4D Flow MRI) analysis of hemodynamics in valve-sparing aortic root repair with an anatomically shaped sinus prosthesis. J Thorac Cardiovasc Surg 2016;152:418-27.e1.
27. Lansac E, Lim HS, Shomura Y, et al. Aortic root dynamics are asymmetric. J Heart Valve Dis 2005;14:400-7.
28. Fries R, Graeter T, Aicher D, et al. In vitro comparison of aortic valve movement after valve-preserving aortic replacement. J Thorac Cardiovasc Surg 2006;132:32-7.
29. Lansac E, Di Centa I, Raoux F, et al. An Expansible Aortic Ring for a Physiological Approach to Conservative Aortic Valve Surgery. J Thorac Cardiovasc Surg 2009;138:718-24.
30. Wuliya M, Sleilaty G, Di Centa I, et al. An expansible aortic ring to preserve aortic root dynamics after aortic valve repair. Eur J Cardiothorac Surg 2015;47:482-90.
31. Lansac E, Di Centa I, Sleilaty G, et al. Remodeling root repair with an external aortic ring annuloplasty. J Thorac Cardiovasc Surg 2017;153:1033-42.
32. Lansac E, Di Centa I, Sleilaty G, et al. Longterm results of external aortic ring annuloplasty for aortic valve repair. Eur J Cardiothorac Surg 2016;50:350-60.

Cite this article as: Lansac E, Lim HS, Shomura Y, Lim KH, Rice NT, Di Centa I, Youssefi P, Goetz W, Duran CM. Aortic valve opening and closure: the clover dynamics. Ann Cardiothorac Surg 2019;8(3):351-361. doi: 10.21037/acs.2019.05.03

